Biomicrofluidics ARTICLE scitation.org/journal/bmf

DNA fragmentation in a steady shear flow

Cite as: Biomicrofluidics 16, 054109 (2022); doi: 10.1063/5.0109361
Submitted: 12 July 2022 · Accepted: 19 September 2022 ·
Published Online: 27 October 2022

Yiming Qiao, Zixue Ma, Clive Onyango, Xiang Cheng, and Kevin D. Dorfman[a)]

AFFILIATIONS

Department of Chemical Engineering and Materials Science, University of Minnesota, Twin Cities, 421 Washington Ave SE, Minneapolis, Minnesota 55455, USA

[a)]**Author to whom correspondence should be addressed:** dorfman@umn.edu

ABSTRACT

We have determined the susceptibility of T4 DNA (166 kilobase pairs, kbp) to fragmentation under steady shear in a cone-and-plate rheometer. After shearing for at least 30 min at a shear rate of 6000 s^{-1}, corresponding to a Reynolds number of $O(10^3)$ and a Weissenberg number of $O(10^3)$, 97.9 $\pm$ 1.3% of the sample is broken into a polydisperse mixture with a number-averaged molecular weight of 62.6 $\pm$ 3.2 kbp and a polydispersity index of 1.29 $\pm$ 0.03, as measured by pulsed-field gel electrophoresis (with a 95% confidence interval). The molecular weight distributions observed here from a shear flow are similar to those produced by a (dominantly extensional) sink flow of DNA and are qualitatively different than the midpoint scission observed in simple extensional flow. Given the inability of shear flow to produce a sharp coil–stretch transition, the data presented here support a model where polymers can be fragmented in flow without complete extension. These results further indicate that DNA fragmentation by shear is unlikely to be a significant issue in microfluidic devices, and anomalous molecular weight observations in experiments are due to DNA processing prior to observation in the device.

I. INTRODUCTION

Microfluidics has played a pivotal role in illuminating the polymer physics of DNA molecules in flow,[1] including the dynamics of tethered polymers,[2–4] the coil–stretch transition,[5,6] elongation of DNA for flow-based mapping,[7,8] and other fundamental questions.[9] The appeal of DNA for studying the dynamics of polymers in flow is threefold. First, owing to its biological origin, DNA is available as a monodisperse system, which greatly simplifies data analysis when compared to polydisperse samples produced by conventional polymer synthesis. Second, bright dyes such as YOYO[10] allow visualizing single DNA molecules with readily available microscopy equipment on time scales well suited to videomicroscopy frame rates. Third, the length scales of DNA are commensurate with microfluidic technologies, with typical radii of gyration ranging from hundreds of nanometers to several micrometers.[11] Taken together, these properties make DNA an attractive model system for studying the properties of polymers in the complex flow fields available in microfluidic devices.

One important challenge in using long DNA as a model polymer is that it is relatively easy to break the molecule in flow. Indeed, even the shear produced by pipetting[12,13] is sufficient to fragment long DNA, and it has been known for decades that manipulating very long molecules (e.g., megabase pair DNA) requires protecting the DNA, either in an agarose plug[14] or converting it to a condensed form.[15] Unfortunately, these protection methods cannot be used for studying DNA in flow. For single-molecule studies, fragmentation of the DNA lowers the throughput, which is a frustrating but solvable problem. In contrast, breaking long DNA in flow becomes a severe issue if one wants to achieve the long-read lengths possible from nanopore sequencing[16] that were ultimately critical to producing a full human genome sequence.[17] The fragility of DNA naturally sets an upper bound for the flow phenomena that can be probed using DNA as a model polymer.

The breakage of DNA in flow has been a subject of study since the discovery of DNA as the genomic carrier of information. Research dating back to the sizing of bacteriophage DNA in the 1960s indicates that (i) shear flows created by high-speed stirring tend to cut DNA close to the midpoint;[18,19] (ii) there is a critical shear rate for cutting DNA of a given molecular weight;[19,20] and (iii) the probability of cutting the dsDNA is a function of the shear rate, not the shear stress.[21] These classic results suggest a hypothesis that, at a given shear rate $\dot{\gamma}$, only DNA sizes $M > M^*$ tend to be cut, and they are cut approximately in half. However, given the precision of the tools available at the time of those experiments,[18–20] the evidence to support such a model of midpoint scission in shear flow is not conclusive, and subsequent experiments in the ensuing

30 years have called this simple model into question. Most notably, experiments on DNA fragmentation in a sink flow[12] produced relatively wide molecular weight distributions that are inconsistent with the latter model. Such wide distributions could emerge from the complexity of the flow field. However, they can also arise from molecular individualism, wherein the dynamics of individual molecules in flow are highly heterogeneous despite all molecules being exposed to the same flow field.[5–22] In either case, the absence of midpoint scission in these later experiments[12] motivates us to revisit the problem of DNA fragmentation in shear using modern rheological and characterization methods.

In the present paper, we examine DNA breakage using the simplest possible flow field: steady shear. We posit that understanding the physics of DNA breakage in this model flow is essential to modeling similar processes in the more complicated flow field possible in microfluidic devices. Indeed, theory[23,24] and single-molecule experiments[25] suggest that the coil–stretch transition driving strong chain extension,[23–26] and ultimately chain scission, is less effective in shear flow than in the stagnation-point extensional flows that tend to produce midpoint scission.[24–30] Moreover, recent microfluidic work on DNA scission in flow has largely focused on the design of funnel-based systems that produce complex flow fields with a mixture of shear and extensional components.[31–35] Engineering such devices first requires a basic model for the breakage of DNA in a simpler flow field, which has not been realized to date.

II. EXPERIMENTAL METHODS

A. DNA preparation

The T4 GT7 DNA molecules [166 kilobase pairs (kbp), Nippon Gene] used in the DNA shear experiments were reacted with T4 ligase to repair any potential nicks along the DNA chains. The loading solution with a DNA concentration of ~ 10 mg/L and 0.5× TBE buffer was prepared by first mixing 7.9 μL of the stock T4 GT7 DNA molecules from the vendor ($\sim$760 mg/L) with 60 μL of T4 DNA ligase reaction buffer (10×, New England Biolabs), 30 μL of 10× Tris base-Boric acid-Ethylenediaminetetraacetic acid (EDTA) (TBE) buffer, 0.6 μL of T4 ligase enzyme (New England Biolabs), and 501.5 μL of water (Millipore Direct-Q3, 18.2 M$\Omega \cdot$ cm at 25 °C). The mixed solution was incubated at 37 °C for 2 h to perform the ligation reaction and was then heated to 65 °C for 20 min to inactivate the T4 ligase enzyme. The resulting solutions were ready to be loaded in the rheometer for the DNA shear experiments.

B. DNA shear experiments

A commercial rotational rheometer in a cone–plate geometry (DHR, TA Instruments) was used to produce a uniform shear rate for the DNA fragmentation experiments. The bottom Peltier plate was fixed and maintained the temperature of the DNA solutions at 20 °C. A rotating steel cone (40 mm diameter, 2° angle) was then equipped with a truncation gap of 50 μm. A solvent trap was applied to provide saturated water vapor and prevent solvent evaporation. To perform the DNA shear experiments, we gradually increased the shear rate from 0 s^{-1} to the desired shear rate (1000, 3000, 5000, or 6000 s^{-1}) in less than 6 s and then maintained that shear rate for the desired time (1, 30, 60, or 120 min). Afterward, the samples were collected using pipet, with a recovery rate of around 90%, for subsequent pulsed-field gel electrophoresis (PFGE) experiments to measure the DNA molecular weight distribution. To control for the breakage of the T4 GT7 DNA molecules from pipetting, we also loaded and unloaded the original T4 GT7 DNA solutions without running the shear experiments.

C. Pulsed-field gel electrophoresis

Pulsed-field gel electrophoresis (PFGE) is a standard method for sizing long DNA and was used in previous experiments[12,29,30] on DNA fragmentation in flow. The collected DNA samples from the DNA shear experiments were first evaporated to a concentration of ~ 50 mg/L prior to running the PFGE. The concentrated DNA solutions were then mixed with a gel loading dye (6×, New England Biolabs). The MidRange PFG markers (New England Biolabs) were used as the molecular weight standards for the PFGE experiments. The dyed DNA samples and the markers were loaded into agarose gels (pulsed-field certified, BioRad) prepared with 0.5× TBE buffer solution and 1% w/v agarose. The experiments were performed using a PFGE system (CHEF-DR II, BioRad) at 14 °C with a 6 V/cm electric field, 5.0 s of initial switching time, 15.0 s of final switching time, and 20 h of total run time. After running the PFGE experiments, the agarose gels were stained with a 0.5 μg/mL ethidium bromide solution (Invitrogen, Thermo Fisher Scientific), illuminated by a UV transilluminator (UVP), and then imaged by a digital camera (Canon PC1250). An example of a PFGE image is shown in Fig. 1.

D. Data processing

The PFGE images were processed by first rotating the image so that the two midrange PFG markers were aligned. The rotated image was then analyzed using a custom-written MATLAB program following the method described in Ref. 36 to output normalized intensity profiles of each lane. An example of a normalized intensity profile for the control experiment in Lane 2 of the PFGE image (Fig. 1) is shown in Fig. 2(a). Since the intensity of stained DNA is proportional to the number of base pairs, the gel images correspond to the weight fraction w_i of molecules with degree of polymerization (or size) M_i, where M_i was obtained through an interpolation of a calibration curve from the markers. The number fraction (x_i) of molecules with size of M_i was then calculated as $x_i = w_i/M_i$ to generate the distribution in Fig. 2(b). The number-averaged molecular weight, M_n, and the weight-averaged molecular weight, M_w, in a given experiment were computed as the averages of distributions of the type in Fig. 2. To provide a facile connection to the PFGE data, we will report M_n and M_w without the conversion factor of 650 g per mole of base pairs, i.e., as number-averaged and weight-averaged degrees of polymerization.

The distribution for w_i also was used to compute the percentage of broken DNA molecules in each lane. Since the data are somewhat noisy and contain two distributions (broken and unbroken DNA), we analyzed them using the following approach. First, the distribution for w_i was transformed using a Box–Cox transformation with a constant exponent value $\lambda = 0.01$; the Box–Cox

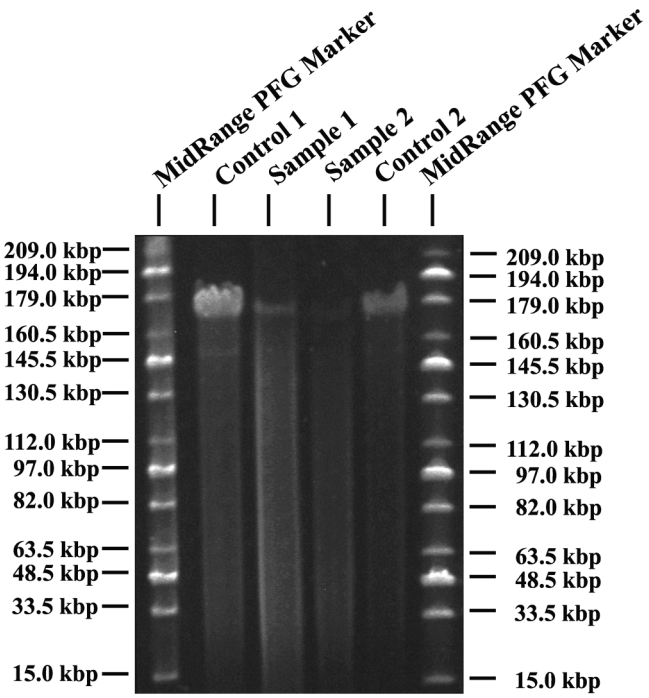

FIG. 1. A typical PFGE image. The MidRange PFG markers are on both sides. The lanes (from left to right) are (i) PFGE marker; (ii) unligated T4 DNA control (loaded and unloaded from the rheometer without any cone rotation); (iii) unligated T4 DNA after being sheared at 6000 s^{-1} for 60 min; (iv) ligated T4 DNA after being sheared at 6000 s^{-1} for 60 min; (v) ligated T4 DNA control; and (vi) PFGE marker.

transformation is a standard method to convert non-Gaussian distributions into approximately Gaussian ones.[36] Afterward, the transformed curves under the broken region, defined as the range of sizes between 15 and 165 kbp, and the unbroken region, defined for sizes between 165 and 209 kbp, were fitted separately using

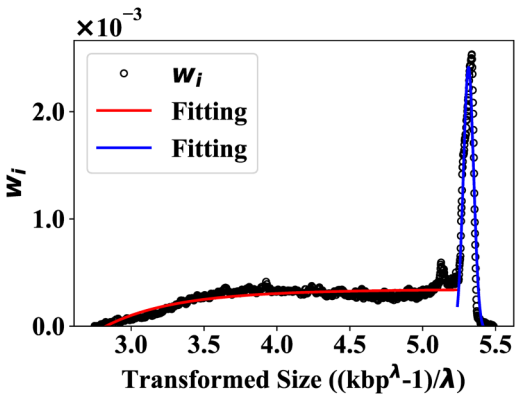

FIG. 3. The Box–Cox-transformed weight-fraction distribution w_i in Fig. 2(a) and the Gaussian-fitted curves for the broken and unbroken parts of the distribution.

Gaussian functions. This cutoff to determine broken vs unbroken DNA was based on the band-broadening that we see for the primary band in the T4 control lane of Fig. 1. Figure 3 provides an example of a transformed weight-fraction distribution and its Gaussian fits. This approach proved to be a robust method for fitting the data across all of our experiments.

To calculate the percentage of broken DNA molecules, the Gaussian fits for the transformed size were converted back to the original molecule sizes, M_i. Then, the percentage of broken DNA molecules ($B_{\%}$), which is the ratio of number of broken molecules to the total number of molecules in each lane, was calculated as

$$B_{\%} = \frac{\int_{15}^{165} M_i w_{fi}\, dM_i}{\int_{15}^{165} M_i w_{fi}\, dM_i + \int_{165}^{209} M_i w_{fi}\, dM_i}, \quad (1)$$

where w_{fi} is the fitted weight fractions obtained from the Gaussian functions (i.e., the two fitting curves in Fig. 3).

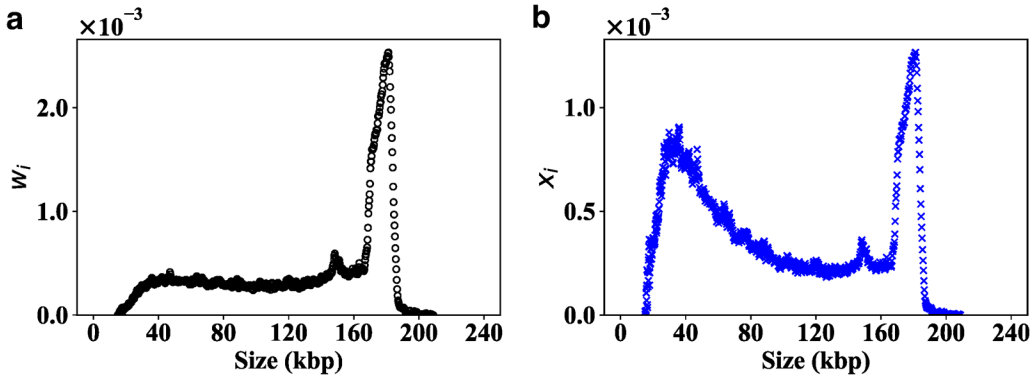

FIG. 2. Molecular weight distributions of T4 DNA control (second lane) in Fig. 1. (a) Weight-fraction distribution w_i. (b) Number-fraction distribution x_i.

III. RESULTS

Our first objective is to determine whether it is even possible to fragment DNA in a steady shear flow. The theory for the coil–stretch transition[23] suggests that this transition is marginal for the Couette flow, and this prediction was supported by single-molecule experimental data.[25] We thus probed the molecular weight distributions produced by 1 h of shearing at shear rates of $\dot{\gamma} = 1000$, 3000, 5000, and 6000s^{-1}. To control for the DNA fragmentation due to the transfer of DNA into and out of the rheometer, as well as the post-processing of the DNA prior to PFGE, we also performed a control experiment where the DNA was loaded into the rheometer but not sheared.

Figure 4 demonstrates that DNA can be significantly fragmented in a steady shear. The control experiment [Fig. 4(a)] shows a strong primary peak at the expected T4 molecular weight of 166 kbp. The breadth of that peak is indicative of the size resolution that we can obtain from PFGE. In the absence of shear, there is a faint band in the gel, corresponding to the plateau in w_i (black circles) from 40 to 160 kbp, which we attribute to DNA processing. As indicated in the supplementary material, pipetting the original sample multiple times does not produce any fragmentation, and the original sample has a bright band at the expected location of 166 kbp (to within the resolution of PFGE). We suspect that the breakage observed in the control experiments arises from extensional flow created during the sample loading and unloading of the rheometer, but additional work would be required to confirm this hypothesis. The detailed mechanism of DNA breakage in the control experiment is tangential to the main focus of our manuscript, and our control experiment is a proper approach to control for the effect shearing the DNA by the rotation of the cone. As such, our discussion of the mechanism of DNA scission in flow will focus on how the primary band at 166 kbp is affected by the flow parameters, keeping in mind that some of the changes in the molecular weight distribution arise from DNA processing independent of those parameters. In particular, we want to assess whether the peak centered at 166 kbp in the control experiment, which represents those DNA that are not broken during processing in the absence of shear, is converted to a new peak at 83 kbp via midpoint scission.

The peak in the number-fraction distribution x_i around 40 kbp in Fig. 4(a) emerges from that plateau in w_i because many small molecules are required to create a fluorescence signal of the same intensity as a few large molecules. The contrast between the control experiment in Fig. 4(a) and the data for $\dot{\gamma} = 6000\,s^{-1}$ in Fig. 4(b) is stark; there is a clear loss of the primary peak at 166 kbp for $\dot{\gamma} = 6000\,s^{-1}$ and a broad distribution in w_i.

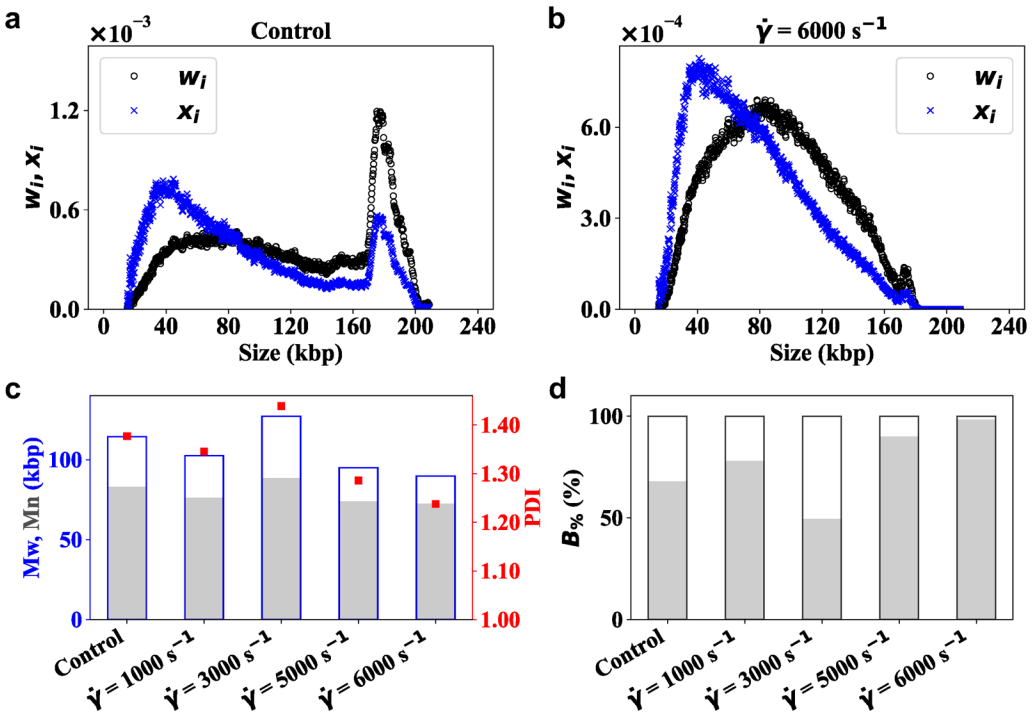

FIG. 4. Data for shearing T4 DNA for 1 h at different shear rates. Data for the number-fraction distribution x_i (blue x) and weight-fraction distribution w_i (black circles) for (a) a control experiment with no shear and (b) a shear rate of $\dot{\gamma} = 6000\,s^{-1}$. The PFGE data used for this figure and molecular weight distributions obtained for other values of $\dot{\gamma}$ are provided in Figs. S1 and S2 in the supplementary material. (c) Weight-averaged molecular weight M_w (white bars with blue edges), number-averaged molecular weight M_n (gray bars), and the polydispersity index PDI (red squares) for different shear rates. (d) Percentage of broken molecules for different shear rates.

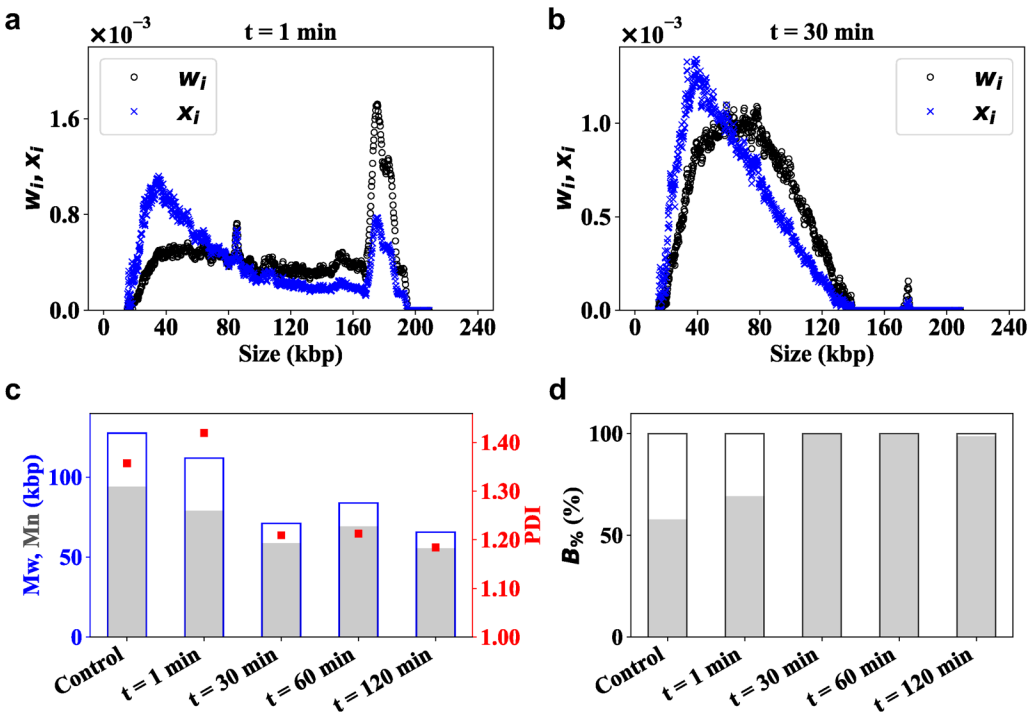

FIG. 5. Data for shearing T4 DNA at $\dot{\gamma} = 6000\,\mathrm{s}^{-1}$ for different shearing times. Data for the number-fraction distribution x_i (blue x) and weight-fraction distribution w_i (black circles) for (a) 1 min of shearing and (b) 30 min of shearing. The PFGE image used for this figure is provided in Fig. S3 in the supplementary material, and additional data for the control (no shear), 60, and 120 min are provided in Fig. S4 in the supplementary material. (c) Weight-averaged molecular weight M_w (white bars with blue edges), number-averaged molecular weight M_n (gray bars), and the polydispersity index PDI (red squares) for different shear rates. (d) Percentage of broken molecules for different shear rates.

Additional data for the lower shear rates, along with the PFGE gel image used for the data analysis, are provided in the supplementary material. The key results are summarized in Fig. 4(c), which compares the weight-averaged molecular weight M_w, the number-averaged molecular weight M_n, and the polydispersity index (PDI = M_w/M_n) for each shear rate and the control experiment, while Fig. 4(d) provides the percentage of broken molecules. At shear rates of $\dot{\gamma} = 1000{-}3000\,\mathrm{s}^{-1}$, there is no appreciable difference between the sheared samples and the control, and we suspect that the minimum in $B_{\%}$ at $3000\,\mathrm{s}^{-1}$ is a statistical fluctuation. Inasmuch as our focus is on cases where essentially all molecules are broken, we chose to fix the shear rate at $\dot{\gamma} = 6000\,\mathrm{s}^{-1}$ for the subsequent experiments.

We then proceeded to determine the time required to fragment the DNA at a shear rate of $\dot{\gamma} = 6000\,\mathrm{s}^{-1}$, using times of 0 (control), 1, 30, 60, and 120 min. The corresponding data for the control and 60 min, which appear in the supplementary material (Figs. S3 and S4) alongside the data for 120 min, serve as replicates for the data presented in Fig. 4; the results are qualitatively the same when comparing the replicates for the controls to one another, and similar qualitative agreement is seen when comparing the replicates for 60 min of shearing to one another. For 1 min of shearing [Fig. 5(a)], the resulting molecular weight distribution is very similar to the control experiment in Fig. 4(a), as well as the additional control experiment appearing in Fig. S4(a) in the supplementary material. Once we reach 30 min of shearing at $\dot{\gamma} = 6000\,\mathrm{s}^{-1}$ in Fig. 5(b), the molecular weight distribution appears similar to the data for 60 min in Fig. 4(b) and the data for 120 min in Fig. S4(d) in the supplementary material. The resulting number-averaged and weight-averaged molecular weights [Fig. 5(c)] and percentage of sheared molecules [Fig. 5(d)] indicate that there is no significant difference between the data after a threshold of 30 min is achieved, while 1 min of shearing has no noticeable impact on the sample when compared to the control.

To assess the reproducibility of the data, we also performed a set of five additional replicates at $\dot{\gamma} = 6000\,\mathrm{s}^{-1}$ for 1 h, as well as a third control experiment. The PFGE data, along with the distributions for x_i and w_i for the replicates, appear in Figs. S5 and S6 in the supplementary material. The summary of the results in Fig. 6 demonstrates that the fragmentation of T4 DNA under these conditions is highly reproducible. To 95% confidence, we find that $97.9 \pm 1.3\%$ of the sample is sheared into a polydisperse mixture with number averaged molecular weight of 66.6 ± 3.2 kbp with a polydispersity index of 1.29 ± 0.03.

One potential issue with DNA fragmentation is the presence of nicks in the DNA. These single-strand breaks are fragile and

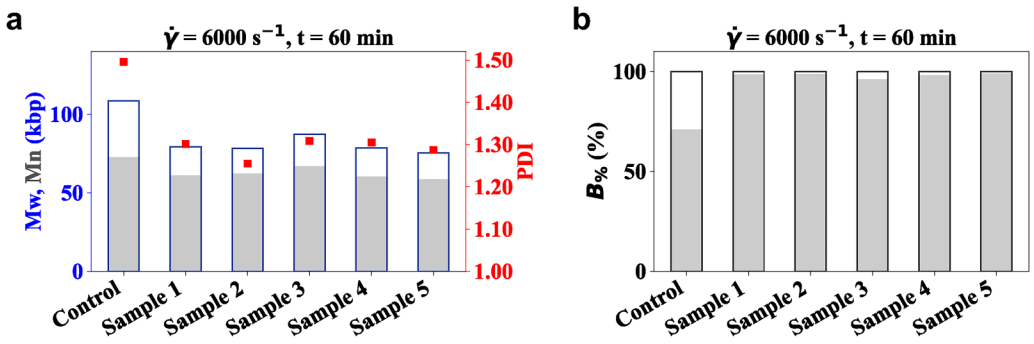

FIG. 6. Reproducibility of the results for shearing at $\dot{\gamma} = 6000\,\mathrm{s}^{-1}$ for 1 h. (a) Weight-averaged molecular weight M_w (white bars with blue edges), number-averaged molecular weight M_n (gray bars), and the polydispersity index PDI (red squares) for a control and different samples under the same shear condition. (b) Percentage of broken molecules for the control and the different sheared samples. The PFGE image used for this figure as well as the distributions for x_i, w_i and the fitting of w_i for each replicate are provided in Figs. S5 and S6 in the supplementary material.

should break more easily than the intact double-stranded DNA. In our experiments, we took a conservative approach by first reacting the DNA sample with T4 DNA ligase, which repairs single strand breaks, prior to shearing. However, as indicated in Fig. S7 in the supplementary material, the ligated and non-ligated samples have similar behavior, indicating that the DNA samples we use are relatively fresh and thus relatively un-nicked.

Since we are using a commercial rheometer for our experiments, we also attempted to detect a stress change in the rheometer that we anticipated would result from the changing molecular weight of the DNA as it fragments. While the apparent viscosity increases when the chains are stretched, it also decreases due to chain scission. In an experiment designed to detect chain stretching in flow, these competing effects are challenging to decouple.[34] As indicated in Fig. S8 in the supplementary material, we saw no significant change in the stress as a function of time when shearing at $\dot{\gamma} = 6000\,\mathrm{s}^{-1}$ for 1 h, while our PFGE data clearly demonstrate that the distribution of DNA molecular weights is shifting during the experiment. Given the low viscosity of the solvent and the very dilute concentrations of DNA, it is unsurprising that we are not able to detect a rheological signature of the DNA fragmentation.

IV. DISCUSSION

Three salient features emerge from our experimental results. First, it is clear that DNA can be fragmented in a shear flow. Second, the time required to achieve a significant amount of fragmentation in shear flow is long, at about 30 min, and only takes place above the critical shear rate $\dot{\gamma}_c \approx 6000\,\mathrm{s}^{-1}$ for the T4 DNA used in our experiments (166 kbp). Third, the location of the scission points appears to be randomly located throughout the molecules, rather than at the midpoint, leading to a broad distribution of molecular weights following processing. In what follows, we discuss each of these key results in the context of the prior literature.

There has been considerable skepticism about the ability to fragment DNA in a linear (Couette) shear flow.[24] The kinematics of a shear flow consists of two parts: an extensional component, which is favorable towards extension and eventual fragmentation, and a rotational component, which leads to tumbling in the flow field[37] that would impede chain scission.[38] Owing to the tumbling motion, de Gennes[23] characterized the coil–stretch transition in Couette flow as marginal, lacking the runaway coupling between extension and hydrodynamic interactions that he predicted produces strong extension of the molecule. Odell and coworkers[24] cast further doubt on the ability of shear flows to fragment polymers because theory predicts that the molecular shape in a shear flow tends to be elliptical. These predictions concerning coil–stretch in shear flows were borne out in single-molecule DNA experiments during parallel plate Couette flow by Smith *et al.*,[25] who observed no sharp coil–stretch transition and, on average, the expected elliptical DNA configuration. The latter experiments[25] further revealed aperiodic fluctuations in the DNA extension whose amplitude and frequency increase with increasing Weissenberg number $\mathrm{Wi} = \dot{\gamma}\tau$, where τ is the longest relaxation time of the DNA. Importantly, the magnitude of the DNA extension saturated at ca. 40%–50% of the maximal extension at the largest values of Wi used in their experiments.[25]

Combining our clear evidence of fragmentation with previous observations of no coil–stretch transition in shear flow[25] leads us to conclude that DNA can be fragmented without reaching full extension. Rabin[39] proposed a mechanism for such a process, wherein the central part of the chain is stretched but the ends are coiled (weakly perturbed). In this model, a polymer can break without achieving full extension because the extension that is critical to fragmentation is that in the highly stretched part the chain. In proposing this mechanism, Rabin[39] aimed to distinguish between (i) fast transient flows, such as a contraction flow, where the residence time in the flow can be shorter than the longest chain relaxation time and (ii) quasi-steady state flows, such as trapping at a stagnation point, wherein a simple extensional flow can be imposed for long times.[6] Linear shear flow can be envisioned as the extreme case of a fast transient flow since tumbling implies that the residence time where the DNA's long axis is also aligned along the extensional axis is short. Our results are also consistent with prior experimental work on flow through an orifice[40] that indicated that DNA can be cleaved without full extension.[39]

To be more quantitative, we find that the shear rate required to achieve fragmentation is very large, $\dot{\gamma}_0 = 6000\,\mathrm{s}^{-1}$. If we estimate the longest relaxation time of T4 DNA in water (viscosity $\eta = 1$ cP) as 1 s,[41] the corresponding Weissenberg number is Wi $\sim$ 1000, much larger than the Wi corresponding to the saturation in DNA extension observed by Smith *et al.*[25] Once the DNA breaks, the degree of polymerization M decreases markedly, and the longest relaxation time decreases accordingly following the scaling $\tau \sim M^{3\nu}$, where $\nu \approx 3/5$ is the Flory exponent, and thus Wi decreases as well. Using a simple model where the DNA fragments in half, we estimate that the Weissenberg number decreases by approximately 70%. The DNA relaxation at this lower Weissenberg number is now too fast to achieve large-amplitude fluctuations needed to produce sufficient tension at the middle of the chain and allow that tension to persist long enough for the bond to break, and the chain fragmentation ceases.

It is curious that the critical shear rate that we observed for T4 DNA (166 kbp), $\dot{\gamma}_c = 6000\,\mathrm{s}^{-1}$, is similar to the critical extension rate, $\dot{\epsilon}_c = 6800\,\mathrm{s}^{-1}$, for fragmenting λ-DNA (48.5 kbp) in an impinging jet setup.[29,30] Given the very different kinematics of pure shear flow and purely extensional flow (as a model of the impinging jet flow), we view this quantitative similarity as coincidental. At best, one might posit that there exists a kinematic rate of $O(10^3)\,\mathrm{s}^{-1}$ that is required to fragment DNA in this approximate molecular weight range.

We found that producing a significant amount of fragmentation requires about 30 min, a time scale that is consistent with prior work in mixed flows[40–42] and the large number of passes required to achieve fragmentation in extensional flow,[28–30] but somewhat longer than the predictions from the coil–stretch theory.[23] An immediate conclusion from this time is that our DNA are not substantially nicked, because nicking would lead to a subset of the DNA to break quickly at the weakened single-strand breaks, only later followed by the double-strand breaks.[12] The latter kinetic argument is also consistent with the insensitivity of our results to ligating the DNA prior to the experiment (Fig. S7 in the supplementary material), which are the expected behavior if the DNA sample is relatively fresh. The physicochemical basis for the long processing time lies in the role of extension on bond breaking, lowering the free energy barrier[23] but still requiring activation over a (now lower energy) transition state. Inasmuch as shear flow at high Wi features high frequency, but also relatively high amplitude fluctuations in the chain extension,[25] it is unsurprising that the fragmentation rate is not very fast; a fluctuation to a large extension needs to be coupled with a second, thermally driven fluctuation over the transition state to fragment the DNA.

Overall, the molecular weight distributions we observed after 1 h of shearing at $\dot{\gamma} = 6000\,\mathrm{s}^{-1}$ are very similar to those observed during a sink flow by Reese and Zimm.[12] The latter experiments used flow of DNA through a hole in a plate to mimic the transient extensional flow that took place during pipetting of DNA, with PFGE used to analyze the resulting molecular weight distribution in a manner analogous to that done here. Similarly, broad molecular weight distributions were measured using size-exclusion chromatography following fast flow of poly(styrene) through an orifice[40] and by gel permeation chromatography following turbulent flow of poly(styrene).[43] These broad molecular weight distributions contrast with those obtained in extensional flows created by four-roll mills, impinging jets, and cross-slot flows of poly(styrene), poly(ethylene oxide), poly(styrene sulfonate), and DNA.[24–30] While the claims of "exact" scission at the polymer midpoint in the latter extensional flows are not supported by the significant spread in the molecular weight distributions[24–30] or the models proposed for chain scission,[30] which predict Gaussian distributions in scission points about the mean, it is clear that extensional flows with a stagnation point lead to qualitatively different fragmentation behavior than even the largely extensional behavior exhibited by a sink flow.[12] The similarities between our results for steady shear flow and the primarily extensional sink flow[12] suggest that the existence of a stagnation point, and the concomitant ability to reach the quasi-steady state flow condition,[39] is a unique flow feature for polymer fragmentation that leads to a relative precision in fragmentation location that cannot be achieved in the presence of even a small amount of vorticity.

The flow field produced by the cone-and-plate rheometer under our conditions is a steady shear flow but may not be a simple shear flow. The cone-and-plate configuration[44] provides a constant shear rate $\dot{\gamma} = \omega/\phi_0$, where ω is the rotation rate of the cone and $\phi_0 = \pi/90$ is the 2° angle between the rotating cone and the stationary plate. The resulting velocity varies from zero at the center to $v = \omega R$ at the edge. The maximum Reynolds number, which would be at the edge of the cone, is thus $\mathrm{Re} = \rho\dot{\gamma}\phi_0^2 R^2/\eta$. Approximating the density ρ and viscosity η of the dilute DNA solution with the density and viscosity of water, this plate-edge Reynolds number is Re $\sim O(10^3)$, which exceeds the Reynolds number Re ≈ 10 where a torque correction is generally required for secondary flow in a cone-and-plate rheometer.[45] For this reason, we cannot definitively rule out the presence of any secondary flows within our system, especially since the presence of the DNA (even as a dilute solution) could produce an elastic instability that could ultimately affect the flow field that produced chain scission.[24] As such, the observations and conclusions we have drawn here are relevant to steady shear flow but not necessarily simple shear flow.

V. CONCLUSIONS

In the present contribution, we have shown that T4 DNA can be fragmented in a steady shear flow at a shear rate of $\dot{\gamma} = 6000\,\mathrm{s}^{-1}$ if the sample is subjected to the flow for 30 min. The resulting molecular weight distributions are reminiscent of those obtained in a sink flow of DNA[12] and markedly different from those obtained in purely extensional flow, where midpoint scission tends to occur.[29,30] Our results have two implications for the basic physics of polymer scission in flow. First, since shear flow is neither expected[23] nor observed[25] to produce a sharp coil–stretch transition, the fragmentation observed in our experiments is consistent with the hypothesis that polymers can be cleaved without complete extension.[39] Second, the comparisons with sink flow and extensional flow indicate that the existence of a stagnation point, which allows the polymer to have long residence time with its major axis aligned with the extensional axis of the flow, is a key criterion for midpoint chain scission; the predominantly extensional flow field in a sink flow yields molecular weight distributions[12] that are closer

to the steady shear observed here than those in a simple extensional flow.[29,30] We have focused here on establishing conditions under which the vast majority of the DNA is broken in the flow. Determining the kinetics of the chain scission requires more finely resolved temporal data than Fig. 5 and could prove a fruitful avenue for further research.

While we have focused here on steady shear flows, it would be interesting to probe DNA scission in time-dependent flows as well. Pre-shearing the DNA is a simple approach, say, starting at 3000s^{-1} and then ramping up to 6000 s^{-1}. Based on the long duration to achieve scission at 6000 s^{-1} and the tumbling dynamics in shear flow, it seems unlikely that pre-shearing would prove effective at increasing the rate of chain scission, but experiments are needed to test this hypothesis. DNA can undergo complex dynamics in oscillatory flows,[46,47] which are likely to be a more robust approach to increase the amount of chain scission.

Our results also have practical implications for microfluidic flows using DNA. We have established an approximate upper bound for the Weissenberg number and minimum bound for residence time that leads to DNA fragmentation in shear flow. Both of these bounds are unlikely to be violated in typical microfluidic experiments but can easily be exceeded in bulk flows. As a result, one still needs to be cautious about DNA fragmentation when handling long DNA prior to injection into a microfluidic device, but the likelihood of in-device fragmentation is low. We can, of course, turn this problem on its head and ask how one might design microfluidic devices that promote controlled DNA fragmentation. Our results clearly indicate that steady shear flows are ineffective for this purpose. Moreover, the similarity in the molecular weight distributions produced by our shear flows and a sink flow[12] suggests that the mixed flows created by contractile geometries, which have been used in several microfluidic experiments,[31–35] are not ideal for producing controlled DNA fragmentation, in particular for targeting midpoint scission because they lack a stagnation point. While simple extensional flow appears to be ideal for DNA fragmentation, microfluidic versions of these flows are best used for manipulation of single molecules,[48] which limits the amount of DNA that could be processed. Identifying a device design that provides controlled DNA fragmentation at a throughput that is sufficient, for example, to meet the needs of long-read DNA sequencing remains an open challenge.

SUPPLEMENTARY MATERIAL

See the supplementary material for images of the PFGE gels for each dataset, plots of the distributions for w_i and x_i for additional experimental conditions and replicates, Gaussian fits to the Box–Cox transform for all experiments, experimental data comparing ligated and un-ligated samples, shear stress data for 6000 s^{-1}, and control experiments for repeated pipetting of T4 DNA.

ACKNOWLEDGMENTS

This work was supported by NIH R21-HG011251. Parts of this work were performed in the Polymer Characterization Facility, University of Minnesota, a member of the NSF-funded Materials Research Facilities Network (www.mrfn.org) via the MRSEC program under NSF DMR-2011401.

AUTHOR DECLARATIONS

Conflict of Interest

The authors have no conflicts to disclose.

Author Contributions

Y.Q. and Z.M contributed equally to this work.

Yiming Qiao: Data curation (equal); Formal analysis (equal); Investigation (equal); Writing – review & editing (supporting). **Zixue Ma:** Data curation (equal); Formal analysis (equal); Investigation (equal); Writing – review & editing (supporting). **Clive Onyango:** Investigation (supporting); Writing – review & editing (supporting). **Xiang Cheng:** Conceptualization (equal); Funding acquisition (equal); Supervision (equal); Writing – review & editing (supporting). **Kevin D. Dorfman:** Conceptualization (equal); Funding acquisition (equal); Supervision (equal); Writing – original draft (lead); Writing – review & editing (lead).

DATA AVAILABILITY

The data that support the findings of this study are openly available in the Data Repository at the University of Minnesota (DRUM, https://conservancy.umn.edu/drum) at the permanent link https://hdl.handle.net/11299/241685, Ref. 49.

REFERENCES

[1]L. Rems, D. Kawale, L. J. Lee, and P. E. Boukany, "Flow of DNA in micro/nanofluidics: From fundamentals to applications," Biomicrofluidics **10**, 043403 (2016).
[2]T. T. Perkins, D. E. Smith, R. G. Larson, and S. Chu, "Stretching of a single tethered polymer in a uniform flow," Science **268**, 83–87 (1995).
[3]P. S. Doyle, B. Ladoux, and J. L. Viovy, "Dynamics of a tethered polymer in shear flow," Phys. Rev. Lett. **84**, 4769–4772 (2000).
[4]C. M. Schroeder, R. E. Teixeira, E. S. Shaqfeh, and S. Chu, "Characteristic periodic motion of polymers in shear flow," Phys. Rev. Lett. **95**, 018301 (2005).
[5]T. T. Perkins, D. E. Smith, and S. Chu, "Single polymer dynamics in an elongational flow," Science **276**, 2016–2021 (1997).
[6]C. M. Schroeder, H. P. Babcock, E. S. G. Shaqfeh, and S. Chu, "Observation of polymer conformation hysteresis in extensional flow," Science **301**, 1515–1519 (2003).
[7]E. Y. Chan, N. M. Goncalves, R. A. Haeusler, A. J. Hatch, J. W. Larson, A. M. Maletta, G. R. Yantz, E. D. Carstea, M. Fuchs, G. G. Wong, S. R. Gullans, and R. Gilmanshin, "DNA mapping using microfluidic stretching and single-molecule detection of fluorescent site-specific tags," Genome Res. **14**, 1137–1146 (2004).
[8]J. W. Griffis, E. Protozanova, D. B. Cameron, and R. H. Meltzer, "High-throughput genome scanning in constant tension fluidic funnels," Lab Chip **13**, 240–51 (2013).
[9]D. J. Mai, C. Brockman, and C. M. Schroeder, "Microfluidic systems for singe DNA dynamics," Soft Matter **8**, 10560–10572 (2012).
[10]H. S. Rye, S. Yue, D. E. Wemmer, M. A. Quesada, R. P. Haugland, R. A. Mathies, and A. N. Giazer, "Stable fluorescent complexes of double-stranded DNA with bis-intercalating asymmetric cyanine dyes: Properties and applications," Nucleic Acids Res. **20**, 2803–2812 (1992).
[11]D. E. Smith, T. T. Perkins, and S. Chu, "Dynamical scaling of DNA diffusion coefficients," Macromolecules **29**, 1372–1373 (1996).
[12]H. R. Reese and B. H. Zimm, "Fracture of polymer chains in extensional flow: Experiments with DNA, and a molecular-dynamics simulation," J. Chem. Phys. **92**, 2650–2662 (1990).

[13]T. T. Perkins, S. R. Quake, D. E. Smith, and S. Chu, "Relaxation of a single DNA molecule observed by optical microscopy," Science **264**, 822–826 (1994).
[14]D. C. Schwartz and C. R. Cantor, "Separation of yeast chromosome-sized DNAs by pulsed field gradient gel electrophoresis," Cell **37**, 67–75 (1984).
[15]R. T. Kovacic, L. Comai, and A. J. Bendich, "Protection of megabase DNA from shearing," Nucleic Acids Res. **23**, 3999–4000 (1995).
[16]M. Jain, S. Koren, J. Quick, A. C. Rand, T. A. Sasani, J. R. Tyson, A. D. Beggs, A. T. Dilthey, I. T. Fiddes, S. Malla, H. Marriott, K. H. Miga, T. Nieto, J. O'Grady, H. E. Olsen, B. S. Pedersen, A. Rhie, H. Richardson, A. Quinlan, T. P. Snutch, L. Tee, B. Paten, A. M. Phillippy, J. T. Simpson, N. J. Loman, and M. Loose, "Nanopore sequencing and assembly of a human genome with ultra-long reads," Nat. Biotechnol. **36**, 338–345 (2018).
[17]S. Nurk, S. Koren, A. Rhie, M. Rautiainen, A. V. Bzikadze, A. Mikheenko, M. R. Vollger, N. Altemose, L. Uralsky, A. Gershman, S. Aganezov, S. J. Hoyt, M. Diekhans, G. A. Logsdon, M. Alonge, S. E. Antonarakis, M. Borchers, G. G. Bouffard, S. Y. Brooks, G. V. Caldas, N.-C. Chen, H. Cheng, C.-S. Chin, W. Chow, L. G. de Lima, P. C. Dishuck, R. Durbin, T. Dvorkina, I. T. Fiddes, G. Formenti, R. S. Fulton, A. Fungtammasan, E. Garrison, P. G. S. Grady, T. A. Graves-Lindsay, I. M. Hall, N. F. Hansen, G. A. Hartley, M. Haukness, K. Howe, M. W. Hunkapiller, C. Jain, M. Jain, E. D. Jarvis, P. Kerpedjiev, M. Kirsche, M. Kolmogorov, J. Korlach, M. Kremitzki, H. Li, V. V. Maduro, T. Marschall, A. M. McCartney, J. McDaniel, D. E. Miller, J. C. Mullikin, E. W. Myers, N. D. Olson, B. Paten, P. Peluso, P. A. Pevzner, D. Porubsky, T. Potapova, E. I. Rogaev, J. A. Rosenfeld, S. L. Salzberg, V. A. Schneider, F. J. Sedlazeck, K. Shafin, C. J. Shew, A. Shumate, Y. Sims, A. F. A. Smit, D. C. Soto, I. Sović, J. M. Storer, A. Streets, B. A. Sullivan, F. Thibaud-Nissen, J. Torrance, J. Wagner, B. P. Walenz, A. Wenger, J. M. D. Wood, C. Xiao, S. M. Yan, A. C. Young, S. Zarate, U. Surti, R. C. McCoy, M. Y. Dennis, I. A. Alexandrov, J. L. Gerton, R. J. O'Neill, W. Timp, J. M. Zook, M. C. Schatz, E. E. Eichler, K. H. Miga, and A. M. Phillippy, "The complete sequence of a human genome," Science **376**, 44–53 (2022).
[18]A. D. Hershey and E. Burgi, "Molecular homogeneity of the deoxyribonucleic acid of phage T2," J. Mol. Biol. **2**, 143–152 (1960).
[19]E. Burgi and A. D. Hershey, "A relative molecular weight series derived from the nucleic acid of bacteriophage T2," J. Mol. Biol. **3**, 458–472 (1961).
[20]L. F. Cavalieri and B. H. Rosenberg, "Shear degradation of deoxyribonucleic acid," J. Am. Chem. Soc. **81**, 5136–5139 (1959).
[21]R. D. Bowman and N. Davidson, "Hydrodynamic shear breakage of DNA," Biopolymers **11**, 2601–2624 (1972).
[22]P. G. de Gennes, "Molecular individualism," Science **276**, 1999–2000 (1997).
[23]P. G. De Gennes, "Coil-stretch transition of dilute flexible polymers under ultrahigh velocity gradients," J. Chem. Phys. **5030**, 5030–5042 (1974).
[24]J. A. Odell, A. J. Muller, K. A. Narh, and A. Keller, "Degradation of polymer solutions in extensional flows," Macromolecules **23**, 3092–3103 (1990).
[25]D. E. Smith, H. P. Babcock, and S. Chu, "Single-polymer dynamics in steady shear flow," Science **283**, 1724–1727 (1999).
[26]R. G. Larson and J. J. Magda, "Coil-stretch transitions in mixed shear and extensional flows of dilute polymer solutions," Macromolecules **22**, 3004–3010 (1989).
[27]A. Keller and J. A. Odell, "The extensibility of macromolecules in solution; A new focus for macromolecular science," Colloid Polym. Sci. **263**, 181–201 (1985).
[28]J. A. Odell and A. Keller, "Flow-induced chain fracture of isolated linear macromolecules in solution," J. Polym. Sci., Part B: Polym. Phys. **24**, 1889–1916 (1986).
[29]T. Atkins and T. Avenue, "Elongational flow studies on DNA in aqueous solution and stress-induced scission of the double helix," Biopolymers **32**, 911–923 (1992).
[30]J. A. Odell and M. A. Taylor, "Dynamics and thermomechanical stability of DNA in solution," Biopolymers **34**, 1483–1493 (1994).
[31]L. Shui, J. G. Bomer, M. Jin, E. T. Carlen, and A. Van Den Berg, "Microfluidic DNA fragmentation for on-chip genomic analysis," Nanotechnology **22**, 494013 (2011).
[32]I. V. Nesterova, M. L. Hupert, M. A. Witek, and S. A. Soper, "Hydrodynamic shearing of DNA in a polymeric microfluidic device," Lab Chip **12**, 1044–1047 (2012).
[33]L. Shui, W. Sparreboom, P. Spang, T. Roeser, B. Nieto, F. Guasch, A. H. Corbera, A. Van Den Berg, and E. T. Carlen, "High yield DNA fragmentation using cyclical hydrodynamic shearing," RSC Adv. **3**, 13115–13118 (2013).
[34]S. Garrepally, S. Jouenne, P. D. Olmsted, and F. Lequeux, "Scission of flexible polymers in contraction flow: Predicting the effects of multiple passages," J. Rheol. **64**, 601–614 (2020).
[35]S. Wu, T. Fu, R. Qiu, and L. Xu, "DNA fragmentation in complicated flow fields created by micro-funnel shapes," Soft Matter **17**, 9047–9056 (2021).
[36]K. Bomsztyk, D. Mar, Y. Wang, O. Denisenko, C. Ware, C. D. Frazar, A. Blattler, A. D. Maxwell, M. B. MacConaghy, and T. J. Matula, "PIXUL-ChIP: Integrated high-throughput sample preparation and analytical platform for epigenetic studies," Nucleic Acids Res. **47**, e69 (2019).
[37]R. Cerf and H. A. Scheraga, "Flow birefringence in solutions of macromolecules," Chem. Rev. **51**, 185–261 (1952).
[38]R. E. Adam and B. H. Zimm, "Shear degradation of DNA," Nucleic Acids Res. **4**, 1513–1538 (1977).
[39]Y. Rabin, "On the mechanism of stretching and breaking of polymers in elongational flows," J. Nonnewton. Fluid Mech. **30**, 119–123 (1988).
[40]T. Q. Nguyen and H. H. Kausch, "Chain scission in transient extensional flow kinetics and molecular weight dependence," J. Nonnewton. Fluid Mech. **30**, 125–140 (1988).
[41]Y. Liu, Y. Jun, and V. Steinberg, "Concentration dependence of the longest relaxation times of dilute and semi-dilute polymer solutions," J. Rheol. **53**, 1069–1085 (2009).
[42]M. Ballauff and B. A. Wolf, "Degradation of chain molecules. 2. Thermodynamically induced shear degradation of dissolved polystyrene," Macromolecules **17**, 209–216 (1984).
[43]A. F. Horn and E. W. Merrill, "Midpoint scission of macromolecules in dilute solution in turbulent flow," Nature **312**, 140–141 (1984).
[44]R. B. Bird, R. C. Armstrong, and O. Hassager, *Dynamics of Polymeric Liquids. Volume 1: Fluid Mechanics* (Wiley, New York, 1987).
[45]C. W. Macosko, *Rheology Principles, Measurements and Applications* (VCH, New York, 1994).
[46]K. Jo, Y. L. Chen, J. J. de Pablo, and D. C. Schwartz, "Elongation and migration of single DNA molecules in microchannels using oscillatory shear flows," Lab Chip **9**, 2348–2355 (2009).
[47]Y. Zhou and C. M. Schroeder, "Transient and average unsteady dynamics of single polymers in large-amplitude oscillatory extension," Macromolecules **49**, 8018–8030 (2016).
[48]A. Shenoy, C. V. Rao, and C. M. Schroeder, "Stokes trap for multiplexed particle manipulation and assembly using fluidics," Proc. Natl. Acad. Sci. U.S.A. **113**, 3976–3981 (2016).
[49]See https://hdl.handle.net/11299/241685 for the data that support the findings of this study.